[Prepared for publication as a Letter in *Langmuir*]

An *In-Situ* Electrochemical Scanning Tunneling Microscopy (ECSTM) Study of Cyanide-Induced Corrosion of Naked and Hexadecyl Mercaptan-Passivated Au(111)

Francis P. Zamborini and Richard M. Crooks*,[1]

Department of Chemistry

Texas A&M University

College Station, TX 77843-3255

[1]e-mail: crooks@chemvx.tamu.edu; fax: 409-845-1399; voice: 409-845-5629

*Author to whom correspondence should be addressed

Submitted: 24 September, 1996

REPORT DOCUMENTATION PAGE

Form Approved
OMB No. 0704-0188

1. AGENCY USE ONLY (Leave blank)	2. REPORT DATE	3. REPORT TYPE AND DATES COVERED
	31 October, 1996	Technical 6/1/96 - 7/31/96

4. TITLE AND SUBTITLE
An *In-Situ* Electrochemical Scanning Tunneling Microscopy (ECSTM) Study of Cyanide-Induced Corrosion of Naked and Hexadecyl Mercaptan-Passivated Au (111)

5. FUNDING NUMBERS
N00014-93-11338
300x084yip
96PR0-1027

6. AUTHOR(S)
F. P. Zamborini, R. M. Crooks

7. PERFORMING ORGANIZATION NAME(S) AND ADDRESS(ES)
Department of Chemistry
Texas A&M University
College Station, Texas 77843-3255

8. PERFORMING ORGANIZATION REPORT NUMBER
23

9. SPONSORING / MONITORING AGENCY NAME(S) AND ADDRESS(ES)
Office of Naval Research
800 North Quincy Street
Arlington, Virginia 22217-5000

10. SPONSORING / MONITORING AGENCY REPORT NUMBER

11. SUPPLEMENTARY NOTES
Submitted for publication in *Langmuir*

12a. DISTRIBUTION / AVAILABILITY STATEMENT
Reproduction in whole, or in part, is permitted for any purpose of the United States Government. This document has been approved for public release and sale; it's distribution is unlimited.

12b. DISTRIBUTION CODE

13. ABSTRACT *(Maximum 200 words)*

In-Situ electochemical scanning tunneling microscopy (ECSTM) was used to study the corrosion of naked and *n* -alkanethiol-modified Au (111) surfaces in basic CN^- solutions. In these studies, the potential of a naked Au electrode is poised at a sufficiently negative value that no electrochemical etching takes place. Small positive potential excursions from the initial potential permit observation of the initial stages of corrosion. The data indicates that initial corrosion of naked Au (111) occurs only at high energy defect sites such as pits and step edges. At slightly higher overpotentials, pitting occurs in the middle of terraces while continuing at step edges. At even higher overpotentials, etching occurs rapidly and uniformly and the surface becomes very rough. Results from this experiment are compared to those obtained after coating the Au surface with a hexadecyl mercaptan self-assembled monolayer (SAM) to determine the extent to which the organomercaptan SAM inhibits Au corrosion. On the SAM-modified Au (111) surface the onset potential for a significant level of etching is shifted several hundred millivolts more positive than on the naked surface. Additionally, the rate of etching is significantly slower and the corrosion process is very different: etching initially occurs on terraces at defect sites within the monolayer instead of on step edges. We determined that potential, rather than time, is the primary factor that controls the rate of corrosion.

14. SUBJECT TERMS	15. NUMBER OF PAGES
	20
	16. PRICE CODE

17. SECURITY CLASSIFICATION OF REPORT	18. SECURITY CLASSIFICATION OF THIS PAGE	19. SECURITY CLASSIFICATION OF ABSTRACT	20. LIMITATION OF ABSTRACT
Unclassified	Unclassified	Unclassified	

ABSTRACT

In-situ electrochemical scanning tunneling microscopy (ECSTM) was used to study the corrosion of naked and *n*-alkanethiol-modified Au(111) surfaces in basic CN^- solutions. In these studies, the potential of a naked Au electrode is poised at a sufficiently negative value that no electrochemical etching takes place. Small positive potential excursions from the initial potential permit observation of the initial stages of corrosion. The data indicate that initial corrosion of naked Au(111) occurs only at high energy defect sites such as pits and step edges. At slightly higher overpotentials, pitting occurs in the middle of terraces while continuing at step edges. At even higher overpotentials, etching occurs rapidly and uniformly and the surface becomes very rough. Results from this experiment are compared to those obtained after coating the Au surface with a hexadecyl mercaptan self-assembled monolayer (SAM) to determine the extent to which the organomercaptan SAM inhibits Au corrosion. On the SAM-modified Au(111) surface the onset potential for a significant level of etching is shifted several hundred millivolts more positive than on the naked surface. Additionally, the rate of etching is significantly slower and the corrosion process is very different: etching initially occurs on terraces at defect sites within the monolayer instead of on step edges. We determined that potential, rather than time, is the primary factor that controls the rate of corrosion.

INTRODUCTION

We report an *in-situ* electrochemical scanning tunneling microscopy (ECSTM) study aimed at better understanding the surface chemistry of naked and hexadecyl mercaptan-modified Au(111) in basic cyanide solutions. Because self-assembled monolayers (SAMs) of organomercaptans strongly adsorb to and passivate metal surfaces such as Au,[1-5] Cu,[5-7] and Ag,[5,8] we thought they might form impervious mass-transfer barriers, thereby providing a simple solution to many corrosion-related problems on the coinage metals. To our knowledge this is the first *in-situ* examination of the corrosion-inhibition properties of organomercaptan SAMs.

ECSTM has been a valuable tool for better understanding electrochemical processes such as corrosion, deposition, and adsorption. High-resolution studies of molecular and atomic adsorbates,[9-12] underpotential deposited (UPD) monolayers,[13-15] and surface restructuring and annealing processes[16-20] on Au substrates have been especially revealing. There are also a number of studies of the oxidation and reduction of Au(111) surfaces that correlate electrochemical data with STM images.[19,21-23] Thus, although there have been many ECSTM studies of inorganic materials on metal surfaces, there have been surprisingly few *in-situ* studies of metals modified with organic monolayers and submonolayers.

Our results show that the presence of the SAM shifts the potential for significant corrosion of Au to potentials several hundred millivolts more positive than its onset on the naked surface. Moreover, the nature of the corrosion process on the

naked and passivated surfaces is different. On unpassivated Au, etching begins at step edges and is quite rapid even at fairly cathodic potentials. On the passivated surface etching begins at defects within the SAM, which mainly occur on terraces. Corrosion expands the original etch pits, but the rate is much slower than on the naked surface. We conclude that while *n*-alkylthiol SAMs reduce the rate of corrosion, they are generally too fragile and contain too many defects to be useful for technological applications in highly corrosive environments.

Electrochemical dissolution of Au in alkaline solutions of CN^- is thought to proceed as shown in equations 1-3:[24-27]

$$Au + CN^- \rightarrow AuCN^-_{ads} \quad (1)$$

$$AuCN^-_{ads} \rightarrow AuCN_{ads} + e^- \quad (2)$$

$$AuCN_{ads} + CN^- \rightarrow Au(CN)_2^- \quad (3)$$

McCarley and Bard studied the dissolution of Au(111) in dilute CN^- solutions at open-circuit potential and found that roughly triangular monolayer etch pits form at atomic defects in the Au.[20] They also found that adsorbed CN^- enhances the mobility of the surface Au atoms.[20] By combining electrochemical methods, STM, and ultrahigh vacuum methods, Sawaguchi *et al.*[28] were able to determine the adlattice structure of AuCN on Au(111). Finally, we have previously discussed how the tip of an STM affects CN^- etching of Au(111), and we used *ex-situ* STM methods to study defects in SAMs using an etch-enhancement technique.[29,30] Our goal in the present study was to use *in-situ* ECSTM to examine the CN^--induced

dissolution of Au(111) under potential control to learn more about the very early stages of Au corrosion and to better understand how inhibiting layers act to reduce the rate of corrosion.

EXPERIMENTAL

Chemicals. Hexadecyl mercaptan $HS(CH_2)_{15}CH_3$ (Aldrich, 92%) was purified by distillation under reduced pressure. KOH (Johnson Matthey, ultrapure), KCN (Fischer, 99.9%), K_2SO_4 (Aldrich, 99%), $Na_2HPO_4 \cdot 6H_2O$ (Mallinkrodt) and 100% Ethanol were used as received. All electrolyte solutions were prepared with deionized water (Millipore, Milli-Q purification system, resistance ≈ 18 MΩ-cm)

Substrate Preparation. SAM-modified substrates were prepared as described previously.[31-36] Briefly, melting a Au wire (0.5-mm diameter, 99.99% purity, Refining Systems Inc., Las Vegas, NV) in a H_2/O_2 flame forms a 1.5-2.0 mm-diameter ball at the end of the wire. The ball has a few elliptical Au(111) facets (long axis ~300 μm) on its surface that contain atomically flat terraces up to 1 μm wide. After fabrication, the balls are electrochemically cleaned and annealed by cycling them in 0.1 M $HClO_4$ between 0.2 V and 1.5 V vs. Ag/AgCl, 3 M NaCl, for 20-30 min at a scan rate of 20 mV/s. SAMs were prepared by placing the Au ball in an ethanolic solution of hexadecyl mercaptan (1-2 mM) for more than 24 h, and then removing it from solution, rinsing with absolute ethanol, and drying under a stream of nitrogen.

STM Data Acquisition. A Nanoscope III electrochemical scanning tunneling microscope (Digital Instruments, Santa Barbara, CA) equipped with an integral potentiostat was used for data

acquisition. The tips were mechanically cut Pt/Ir (80/20, Digital Instruments, Santa Barbara, CA) and coated with apiezon wax to minimize Faradaic leakage current, which was generally 10-20 pA (measured by cycling the tip between +0.1 V and -0.1 V vs. a Pt wire in 0.1 M KCl at 100 mV/s). The electrochemical cell was fabricated from Kel-F and held a large enough volume (22-25 mL) that there was no danger of exhausting reagents (such as CN^-), which might occur in the very low-volume cells typically used for ECSTM studies. The large cell volume also accommodates a true reference electrode (Ag/AgCl, 3 M NaCl, BAS, West Lafayette, IN) against which all potentials are reported. A salt bridge consisting of a fritted tube filled with 0.1 M K_2SO_4 served to protect the reference electrode from CN^- and the Au surface from Cl^- contamination. A Pt wire counter electrode completed the cell. All electrolyte solutions were air saturated.

All STM images were obtained in the constant-current mode. Other relevant conditions, including the grey scale (z), the tunneling current (i_t), the scan size, the substrate potential (E_{sub}), the tip-substrate bias potential (E_{bias}), time the surface was poised at the indicated potential (t_{pot}), total time of the experiment, which is defined as the time elapsed between when the substrate potential is moved from -900 mV (Frame a in each figure) until the end of frame capture of subsequent images (t_{tot}), and the root-mean-square (RMS) roughness values are noted in the figures or figure captions. A positive value of E_{bias} means the tip potential is positive of E_{sub}.

RESULTS AND DISCUSSION

CN^- etching of nominally naked Au(111). Figure 1 shows a series of 1 x 1 μm images obtained at different electrochemical potentials from a Au(111) surface immersed in a solution containing 10 mM KCN and pH 11 phosphate buffer (0.1 M). Au etches at its open-circuit potential in O_2-saturated CN^- solution, so the substrate was introduced into the electrolyte solution under potential control at -1.0 V where it is cathodically protected and no etching occurs. Figure 1a shows the Au(111) surface at -900 mV where no noticeable dissolution occurred for up to 3.0 min, because it is still cathodically protected at this potential.

Figure 1

When the electrode potential is stepped to -850 mV, corrosion is very slow and occurs primarily at step edges (Figure 1b), although a few pits appear on the terraces. Figure 1c shows the surface at -800 mV where etching proceeds rapidly, but is still emanating from the step edges. At -700 mV (Figure 1d) the surface once again appears smooth, but this is an effect of the scanning tip, which we have noticed before,[29] and it is not representative of the entire surface. To gain more representative images under these rapid etching conditions we imaged a nearby region of the surface at -500 mV (Figure 1e). The surface looks much rougher and is characterized by numerous spherical Au crystallites ranging from 30-70 nm in diameter. Figure 1f, which was obtained at -400

mV in the same region as Figure 1e, indicates further corrosion of the surface. The tip position was offset before capturing the images at -200 mV (Figures 1g and 1h) to minimize image distortion by the scanning tip. The Au surface continues to roughen at these extreme potentials and the surface no longer consists of the well-defined Au crystallites shown in Figures 1e and 1f. Enhanced etching at more positive potentials is also reflected in the root-mean-square (RMS) roughness of the surface, which increases from 5.9 nm in Figure 1e to 13.8 nm in Figure 1h. Taken together, these images indicate that corrosion begins primarily on step edges and that the rate of corrosion and surface morphology are defined by the electrochemical potential of the surface.

CN^- etching of Hexadecyl Mercaptan-Modified Au(111). Figure 2 shows a series of 1 x 1 μm images of a hexadecyl mercaptan-modified Au(111) surface at various potentials and in contact with an electrolyte solution identical to that used for the naked-Au etching experiment just described. The Au substrate was introduced into the solution at -900 mV, rather that -1.0 V, to prevent electrochemical desorption of the mercaptan, which may occur at more negative potentials.[37] Figure 2a shows that some

Figure 2

etch pits have already formed at -900 mV even though we did not observe etching on the naked Au surface at this potential. Contamination of the nominally naked Au and the fact that the SAM-modified surface was at this potential almost 7 min longer could

account for this observation. The etch pits are most likely points where defects in the monolayer permit intimate contact between CN^- and the Au surface, which is a necessary condition for etching.

Unfortunately, we found that the STM tip damages the SAM surface upon extensive scanning, and therefore it is not possible to obtain reliable information about surface passivation from exactly the same region of the surface. Rather, it was necessary to change the locations after each image in Figure 2. Although this situation is less than ideal, it is possible to identify some definite trends in the progression of the etch pits. As etching proceeds, the density, width, and depth of the pits increase. The pits indicated by the arrows in Figures 2a, 2b, and 2c are all roughly the same diameter (31.4 nm, 30.0 nm, and 31.9 nm, respectively), but their depth increases with increasing etching time and potential (6.5 Å, 13.6 Å, and 24.0 Å, respectively). Because these three etch pits are all about the same width, but increasing in depth, we believe that etching proceeds preferentially downward into the Au at low overpotentials (up to -700 mV). At more positive overpotentials, as in Figures 2d-2g, the pits also etch outward at a significant rate. This result is consistent with our general conclusion that the SAM inhibits, but does not prevent, Au dissolution.

It is interesting to note that etching first appears mostly on the terraces for the SAM-coated surface. This is in contrast to the observation that on the naked Au surface etching first occurs along step edges. We think that the SAMs adsorb onto the

Au at the step edges more strongly than the terraces because the former are higher energy sites. This observation is consistent with previous observations that SAMs passivate better on rougher Au surfaces[38] and that other adsorbates that coordinate through metal-sulfur interactions bond preferentially at step edges.[39] Alternatively, the SAMs may nucleate first at step edges and then grow outward into the terraces where defects in packing are present at phase-domain boundaries.

Figures 2d and 2e show the surface at -600 mV and -500 mV respectively. The number density of etch pits has increased from about 12/μm^2 in Figure 2c to 24/μm^2 in Figure 2e. They are also much wider (50-100 nm) and deeper (> 35 Å) and have grown into very well-defined triangular and hexagonal shapes in Figure 1e, reflecting the symmetry of the underlying Au(111) surface.[30] At -400 mV (Figure 2f) and -200 mV (Figure 2g), the pits coalesce as they continue to become wider and deeper.

When comparing the images of the SAM-modified Au surface to those obtained on the nominally naked Au, it is clear that the SAM decreases the corrosion rate considerably. This is demonstrated by comparing the RMS roughness values of images obtained at the same potential (Figures 2e, 2f, and 2g with Figures 1e, 1f, and 1g). Figures 1e and 2e were both obtained at E_{sub}=-500 mV and similar t_{tot}, but the RMS roughness on the naked Au is 5.94 nm compared to 0.86 nm on the SAM-modified Au. Similarly, the RMS roughness values for the naked Au at E_{sub}=-400 mV (6.20 nm) and -200 mV (13.7 nm) are much larger than for the SAM-modified Au at the same potentials (3.15 nm and 4.19 nm respectively)

As mentioned previously, it was not possible to reliably image the same area throughout the experiment because of the effect of the tip on the monolayer. The SAM is ~23 Å[40] thick and significant electron tunneling can probably only occur through distances of ~10 Å under the conditions used here, therefore it is likely that the tip pushes through the monolayer while scanning. This probably disrupts the film, allows CN^- to penetrate, and thereby enhances etching under the tip. Figure 2h clearly demonstrates this effect. The 8 approximately 1 x 1 μm areas marked are those scanned during this experiment. These features are 30-50 nm deep.

The images shown in Figure 2 convolute time and electrode potential. That is, both time and potential change in the sequence of images. To confirm our hypothesis that etching is governed principally by potential, we obtained a series of 900 x 900 nm images (Figure 3) of a hexadecyl mercaptan-modified Au(111) surface in contact with an electrolyte solution identical to that used for the two previously described experiments (Figures 1 and

Figure 3

2). The Au substrate was introduced into the electrochemical cell at -900 mV and then stepped to -700 mV, where images were captured at constant potential, but at different times. The times given in the figure are referenced to the instant before the substrate is stepped to -700 mV. At -900 mV (Figure 3a) some etch pits have already formed, as in Figure 2a. The images in Figures 3b-3f show

that minimal etching occurs for up to 23.8 min at -700 mV, although most of the pits enlarge slightly and a few new pits form (indicated by the circles in Figures 3b and 3f). By comparing the topography of Figures 2g and 3f, which we obtained at roughly the same times (20.5 and 23.8 min, respectively) but very different potentials (-200 and -700 mV, respectively), we conclude that electrode potential is the dominant factor affecting the rate of corrosion.

CONCLUSIONS

We have demonstrated that the rate of Au(111) corrosion on an organomercaptan-modified surface is slower than on a nominally naked Au surface. However, the SAM-modified surface only passivates the surface well at quite negative potentials, and even then etching at defect sites within the SAM proceeds at a fairly rapid rate. The mechanism of corrosion on the naked Au(111) is different from that of the hexadecyl mercaptan-modified surface. Initially, the naked surface etches at high energy sites such as step edges while the SAM-modified surface etches at SAM-defect sites on terraces. The naked Au(111) then etches more rapidly and uniformly to yield circular crystallites; eventually the surface becomes very rough. The SAM-modified Au(111) etches out from defect sites to form triangular and hexagonal-shaped pits. The extent of etching on the SAM-modified surface depends primarily on substrate potential rather than time; at modestly positive potentials the rate of etching is slow. Overall, the SAM-modified surface is more resistant to corrosion for longer periods of time

and at more positive (etching) potentials than the nominally naked surface.

We conclude that even under the best of circumstances, however, *n*-alkanethiol SAMs are insufficiently stable and contain too many defect sites to be technologically useful corrosion inhibitors for most applications. At the present time we are exploring the use of polymerizable SAMs[41,42] as more effective corrosion inhibitors.

ACKNOWLEDGMENTS

We gratefully acknowledge the Office of Naval Research for full financial support of this work.

REFERENCES

(1) Chailapakul, O.; Sun, L.; Xu, C.; Crooks, R. M. *J. Am. Chem. Soc.* **1993**, *115*, 12459-12467.

(2) Chidsey, C. E. D.; Loiacono, D. N. *Langmuir* **1990**, *6*, 682-691.

(3) Michelhaugh, S. L.; Bhardwaj, C.; Cali, G. J.; Bravo, B. G.; Bothwell, M. E.; Berry, G. M.; Soriaga, M. P. *Science* **1991**, *47*, 322-328.

(4) LaGraff, J. R.; Gewirth, A. A. *J. Phys. Chem.* **1995**, *99*, 10009-10018.

(5) Laibinis, P. E.; Whitesides, G. M. *J. Am. Chem. Soc.* **1992**, *114*, 1990-1995.

(6) Laibinis, P. E.; Whitesides, G. M. *J. Am. Chem. Soc.* **1992**, *114*, 9022-9028.

(7) Itoh, M.; Nishihara, H.; Aramaki, K. *J. Electrochem. Soc.* **1995**, *142*, 3696-3704.

(8) Li, W.; Virtanen, J. A.; Penner, R. M. *Langmuir* **1995**, *11*, 4361-4365.

(9) Gao, X.; Weaver, M. J. *J. Am. Chem. Soc.* **1992**, *114*, 8544-8551.

(10) Tao, N. J.; Lindsay, S. M. *J. Phys. Chem.* **1992**, *96*, 5213-5217.

(11) McCarley, R. L.; Bard, A. J. *J. Phys. Chem.* **1991**, *95*, 9618-9620.

(12) Batina, N.; Yamada, T.; Itaya, K. *Langmuir* **1995**, *11*, 4568-4576.

(13) Magnussen, O. M.; Hotlos, J.; Nichols, R. J.; Kolb, D. M.; Behm, R. J. *Phys. Rev. Lett.* **1990**, *64*, 2929-2932.

(14) Stimming, U.; Vogel, R.; Kolb, D. M.; Will, T. *J. Power Sources* **1993**, *43-44*, 169-180.

(15) Manne, S.; Hansma, P. K.; Massie, J.; Elings, V. B.; Gewirth, A. A. *Science* **1991**, *251*, 183-186.

(16) Gao, X.; Hamelin, A.; Weaver, M. J. *J. Chem. Phys.* **1991**, *95*, 6993-6996.

(17) Tao, N. J.; Lindsay, S. M. *J. Appl. Phys.* **1991**, *70*, 5141-5143.

(18) Tao, N. J.; Lindsay, S. M. *Surf. Sci. Lett.* **1992**, *274*, L546-L553.

(19) Trevor, D. J.; Chidsey, C. E. D.; Loiacono, D. N. *Phys. Rev. Lett.* **1989**, *62*, 929-932.

(20) McCarley, R. L.; Bard, A. J. *J. Phys. Chem.* **1992**, *96*, 7410-7416.

(21) Wiechers, J.; Twomey, T.; Kolb, D. M. *J. Electroanal. Chem.* **1988**, *248*, 451-460.

(22) Honbo, H.; Sugawara, S.; Itaya, K. *Anal. Chem.* **1990**, *62*, 2424-2429.

(23) Vitus, C. M.; Davenport, A. J. *J. Electrochem. Soc.* **1994**, *141*, 1291-1298.

(24) MacArthur, D. M. *J. Electrochem. Soc.* **1972**, *119*, 672.

(25) Kirk, D. W.; Foulkes, F. R. *J. Electrochem. Soc.* **1980**, *127*, 1993-1997.

(26) Kirk, D. W.; Foulkes, F. R.; Graydon, W. F. *J. Electrochem. Soc.* **1978**, *125*, 1436-1443.

(27) Cathro, K. J.; Koch, D. F. A. *J. Electrochem. Soc.* **1964**, *111*, 1416-1420.

(28) Sawaguchi, T.; Yamada, T.; Okinaka, Y.; Itaya, K. *J. Phys. Chem.* **1995**, *99*, 14149-14155.

(29) Li, Y.; Chailapakul, O.; Crooks, R. M. *J. Vac. Sci. Technol. B* **1995**, *13*, 1-7.

(30) Sun, L.; Crooks, R. M. *Langmuir* **1993**, *9*, 1951-1954.

(31) Chailapakul, O.; Crooks, R. M. *Langmuir* **1993**, *9*, 884-888.

(32) Hsu, T.; Cowley, J. M. *Ultramicroscopy* **1983**, *11*, 239-250.

(33) Ross, C. B.; Sun, L.; Crooks, R. M. *Langmuir* **1993**, *9*, 632-636.

(34) Schoer, J. K.; Ross, C. B.; Crooks, R. M.; Corbitt, T. S.; Hampden-Smith, M. J. *Langmuir* **1994**, *10*, 615-618.

(35) Snyder, S. R. *J. Electrochem. Soc.* **1992**, *139*, 5C.

(36) Sun, L.; Crooks, R. M. *J. Electrochem. Soc.* **1991**, *138*, L23-L25.

(37) Widrig, C. A.; Chung, C.; Porter, M. D. *J. Electroanal. Chem.* **1991**, *310*, 335-359.

(38) Creager, S. E.; Hockett, L. A.; Rowe, G. K. *Langmuir* **1992**, *8*, 854-861.

(39) Frank, E. R.; Chen, X. X.; Hamers, R. J. *Surface Science* **1995**, *334*, L709-L714.

(40) Porter, M. D.; Bright, T. B.; Allara, D. L.; Chidsey, C. E. D. *J. Am. Chem. Soc.* **1987**, *109*, 3559-3568.

(41) Kim, T.; Chan, K. C.; Crooks, R. M.; Ye, Q.; Sun, L. *Langmuir* in press.

(42) Kim, T.; Chan, K. C.; Crooks, R. M. *J. Am. Chem. Soc.*

FIGURE CAPTIONS

Figure 1. Sequence of ECSTM images of bare Au(111) in 10 mM KCN + pH 11 buffered Na_2HPO_4. i_t = 15 nA in all images. E_{sub} is noted in image.

Image	t_{pot} (min)	t_{tot} (min)	Size (μm)	E_{bias} (mV)	Z (nm)	RMS (nm)
a	3.0	0.0	1	600	2	0.11
b	3.0	3.0	1	600	2	0.10
c	1.3	4.4	1	500	2	0.33
d	1.2	7.3	1	500	2	0.27
e	1.3	13.5	1	300	50	5.9
f	1.1	14.7	1	300	50	6.2
g	1.4	16.3	1	100	80	13.7
h	2.6	17.5	1	100	80	13.8

Figure 2. Sequence of ECSTM images of hexadecyl mercaptan-modified Au(111) in 10 mM KCN + pH 11 buffered Na_2HPO_4. i_t = 10 nA in all images. E_{sub} is noted in image.

Image	t_{pot} (min)	t_{tot} (min)	Size (μm)	E_{bias} (mV)	Z (nm)	RMS (nm)
a	9.8	0.0	1	100	2	0.10
b	1.5	1.5	1	100	2	0.12
c	1.6	4.5	1	100	2	0.16
d	2.9	8.9	1	100	2	0.35
e	2.8	11.8	1	100	5	0.86
f	3.3	15.3	1	100	30	3.2
g	1.6	20.5	1	100	35	4.2
h	4.4	23.2	14	100	50	9.5

Figure 3. Sequence of ECSTM images of hexadecyl mercaptan-modified Au(111) in 10 mM KCN + pH 11 buffered Na_2HPO_4. The electrode was poised at -700 mV for the time durations indicated in the figure. (a) was obtained at E_{sub} = -900 mV; (b)-(g) were obtained at E_{sub} = -700 mV.

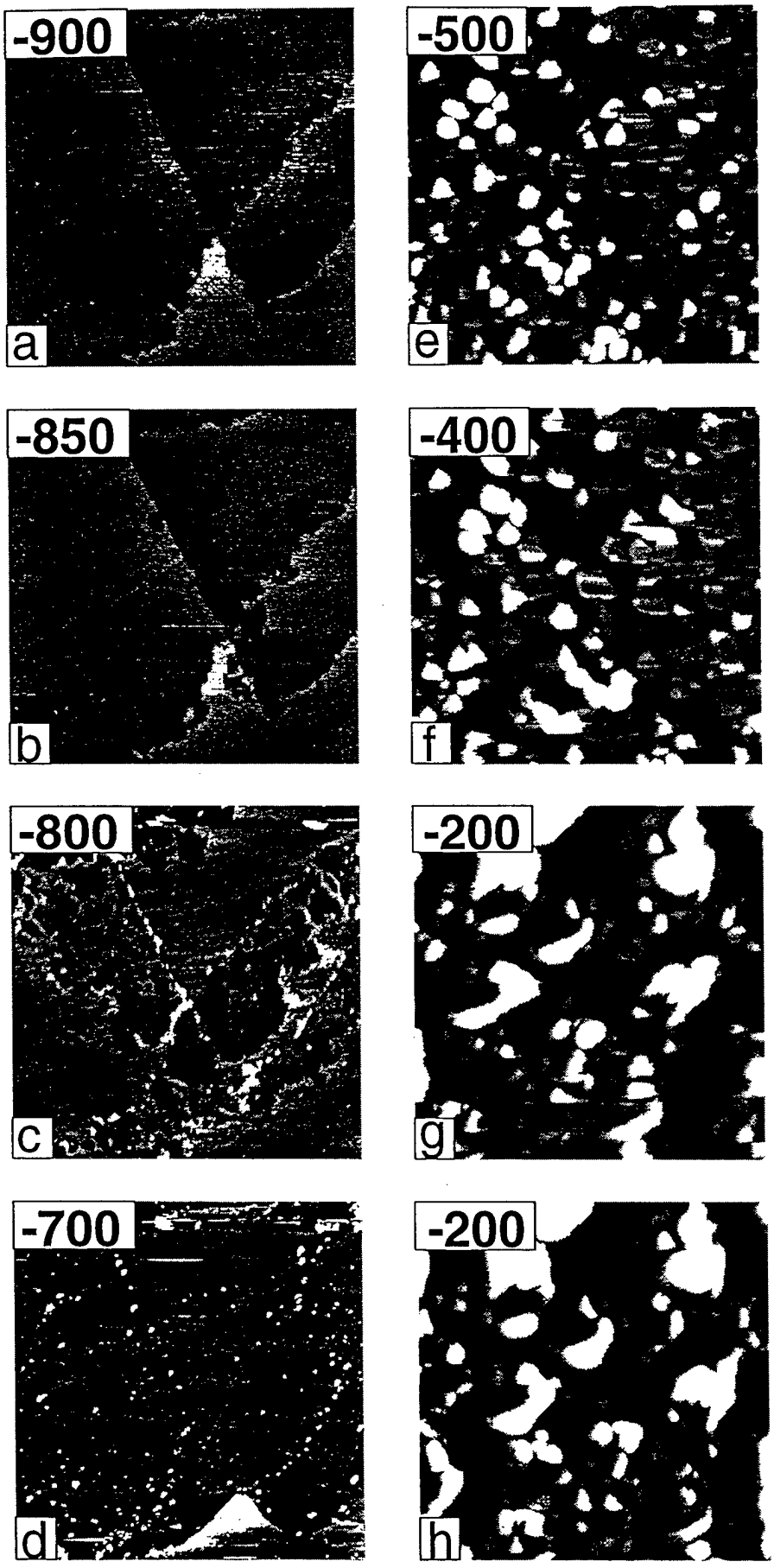

Figure 1, Zamborini and Crooks

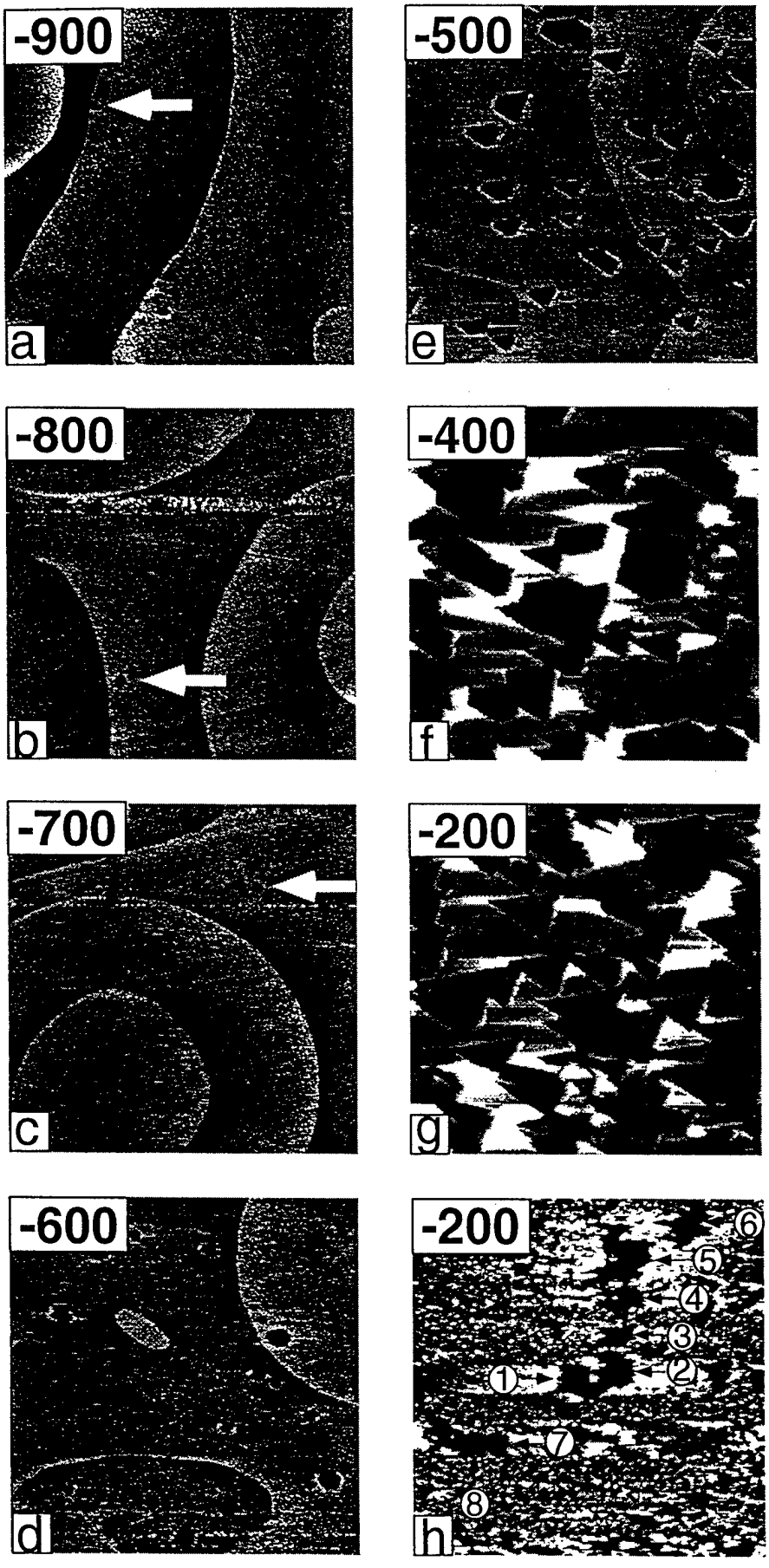

Figure 2, Zamborini and Crooks

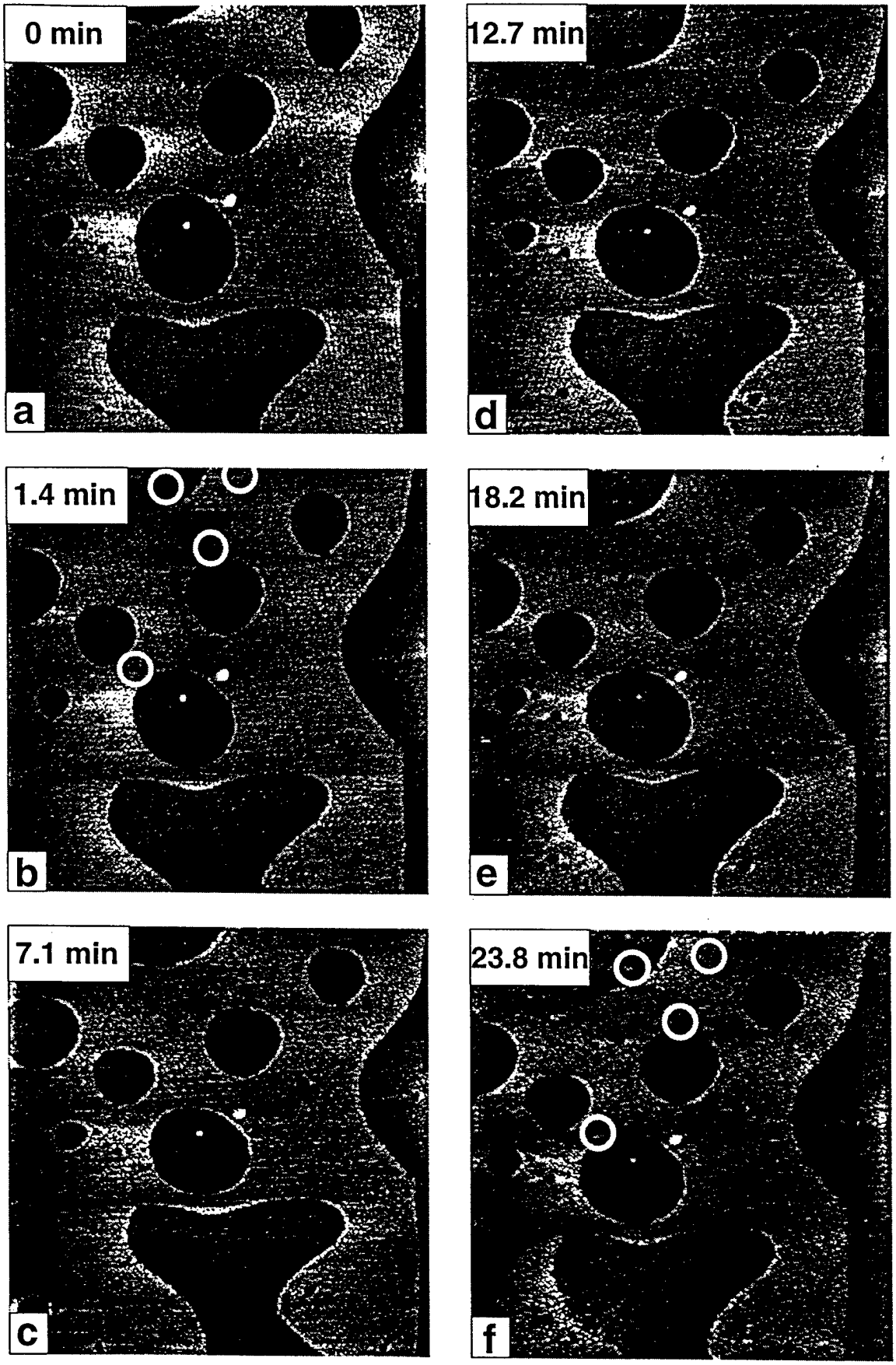

Figure 3, Zamborini and Crooks